# Numerical simulation of fibre reorientation in the consolidation of a continuous fibre composite material

A.B.Wheeler and R.S.Jones
Department of Mathematics
University of Wales
Aberystwyth
Dyfed
SY23 3BZ

**Abstract**

When a rectangular sample of aligned, continuous, fibre-reinforced composite is subjected to normal pressure it has been observed that resin is squeezed out parallel to the fibres and the fibres flow transversely. The fibres deform so that the sample becomes 'barrel' shaped. A three-dimensional code has been developed to simulate this flow.

The material is modelled as an Ericksen, transversely isotropic continuum in which the fibre direction is specified at each point by a vector **a**. The system of coupled equations are solved using a finite-difference technique. The transverse and longitudinal viscosities are assumed to be functions of the fibre volume fraction which increases as the resin is forced to percolate parallel to the fibres.

The stress equations of motion are discretised using central differences for a fixed orientation and the discretised equations solved using a pseudo-time technique. The converged solution is then used to determine the change in fibre direction at each point of the continuum. The process is repeated in real time using the new fibre orientation. In the momentum equations the viscous terms are treated explicitly and the pressure gradient implicitly. A projection method is used to ensure that the mass is conserved at each time step. The results are in broad agreement with the experimental observations and demonstrate the success of the continuum model to predict flow behaviour.

## Introduction

Fibre reinforced composite materials consist of a matrix reinforced with fibres. These fibres may be either continuous or discontinuous, flexible or rigid. In the forming of the materials the matrix, in its molten state, flows and transports the fibres which in turn constrain the flow. The properties of the finished product will depend on the final position and alignment of these fibres. It is of interest, therefore, to be able to simulate these flows and predict the motion of the fibres.

In this paper we model the composite as an anisotropic continuum in which the fibre direction at any point is described by a vector **a**. In 1960 Ericksen [1] derived a general form for a class of

constitutive equations for incompressible transversely isotropic fluids. More recently special cases this model have been used to represent continuous fibre-reinforced composite [2-5].

For all but the simplest flow geometries a numerical approach is necessary to deal with the complexities of the equations and the boundary conditions. Finite element schemes have been developed for modelling composite sheet forming processes [6].

In the present work the governing equations are discretised on a general uniform grid using finite difference scheme. The resulting system of equations are solved iteratively using a time marching technique based on the ideas of Chorin [7].

During the deformation process resin is squeezed out parallel to the fibres causing an increase in the volume fraction, on which the transverse and longitudinal viscosities have been observed to be dependent, [8]. In this paper we represent the viscosity dependence using the analytical model proposed by Christensen [9], which was shown to be in good agreement with results from experiments on a model system [8].

## Basic Equations

The composite, in its melt state, is described as an anisotropic incompressible liquid having at each point a single preferred direction represented by a unit vector **a**. Following Ericksen [1], it can be shown that the most general linear relationship between the stress $\sigma$ and the rate of strain **d** is

$$\sigma = -p\mathbf{I} + 2\eta_T\mathbf{d} + 2(\eta_L - \eta_T)(\mathbf{aa}.\mathbf{d} + \mathbf{d}.\mathbf{aa}) + \mu_0\mathbf{aa} + E_L\mathbf{d} : \mathbf{aaaa}, \tag{1}$$

$$\mathbf{d} = \frac{1}{2}(\nabla\mathbf{u} + \nabla\mathbf{u}^T), \tag{2}$$

where p is the isotropic pressure and **u** is the velocity vector, $\mu_0$ represents a tension in the fibre direction, $\eta_L$ and $\eta_T$ represent shear viscosities and $E_L$ represents an elongational viscosity in the fibre direction.

The vector **a** occurs explicitly in (1) and an extra dynamic equation must be provided to determine its rate of change d**a**/dt. The most general relationship that gives d**a**/dt in terms of **a** and **d**, which is linear in $\nabla\mathbf{u}$ and satisfies $\mathbf{a}.\mathbf{a} = 1$, is

$$\frac{\partial\mathbf{a}}{\partial t} + \mathbf{u}.\nabla\mathbf{a} = \frac{1}{2}\{(1+\lambda)\mathbf{a}.\nabla\mathbf{u} + (\lambda - 1)\mathbf{a}.\nabla^T\} - \lambda\mathbf{aaa} : \nabla\mathbf{u}, \tag{3}$$

where $\lambda$ is a constant. In the present paper we take $\lambda = 1$ and $\mu_0 = 0$ which is an appropriate form for continuous fibre reinforced materials.

The two shear viscosities $\eta_L$ and $\eta_T$ are assumed to depend on volume fraction f. Following Christensen [9] we take

$$\frac{\eta_L}{\eta_m} = \frac{1 + 0.873\bar{f}}{(1-0.8815\bar{f})^{1/2}(1-\bar{f})^{1/2}}, \tag{4}$$

$$\frac{\eta_r}{\eta_m} = \frac{(1+0.193\bar{f})^3}{(1-0.5952\bar{f})^{3/2}(1-\bar{f})^{3/2}}, \tag{5}$$

where $\bar{f} = (2\sqrt{3}/\pi)f$ $(0 \le f \le \pi/2\sqrt{3})$ and $\eta_m$ is the matrix viscosity. Christensen's model is a semi-empirical model which conforms to theoretical results for dilute and concentrated suspensions.

It can at this point, be noted that the special case of the Newtonian constitutive equation can be obtained by taking $\mathbf{a} = \mathbf{0}$.

Incompressibility imposes the constraint

$$\nabla.\mathbf{u} = 0. \tag{6}$$

The materials are highly viscous and it is assumed that the inertia terms can be neglected so that the equations of motion become

$$\nabla.\sigma = 0. \tag{7}$$

## Numerical Technique

The governing equations are discretised in time using a splitting scheme originally due to Chorin [7]. This procedure can be used either to obtain a transient solution or as the basis of an iterative method to reach the steady state solution. At each new time step the pressure is determined so that the new velocity field is divergence free. For steady state calculations the time step $\Delta t$ may be regarded as a relaxation parameter. If $\mathbf{u}^{(n)}$ denotes the velocity field at time $t = n\Delta t$, then the splitting scheme may be written as

$$\frac{\mathbf{u}^* - \mathbf{u}^{(n)}}{\Delta t} = \nabla.\mathbf{T}^{(n)}, \tag{8}$$

$$\frac{\mathbf{u}^{(n+1)} - \mathbf{u}^*}{\Delta t} = -\nabla.p^{(n+1)}, \tag{9}$$

$$\nabla.\mathbf{u}^{(n+1)} = 0. \tag{10}$$

In addition the prescribed boundary conditions are imposed on $\mathbf{u}^{(n+1)}$. The stress term in the momentum equation is treated explicitly. The variable $\mathbf{u}^*$ is an intermediate velocity which is introduced for computational convenience rather than for any physical reason.

We take the divergence of (9) and use (10) to obtain a Poisson equation for $p^{(n+1)}$:

$$\nabla^2.p^{(n+1)} = \frac{\nabla.\mathbf{u}^*}{\Delta t}. \tag{11}$$

We begin the method by prescribing some initial velocity field $u^{(0)}$. Each step of the algorithm proceeds as follows:

(a) Determine $\mathbf{u}^*$ from (8).

(b) Solve the Poisson equation (11) for $p^{(n+1)}$ using the normal component of (9) to obtain a Neumann boundary condition on the solid walls and $\sigma.\mathbf{n} = 0$ on the free surface.

(c) Determine $u^{(n+1)}$ using (9).

The only implicitness in the algorithm is the determination of the pressure. This stage requires the solution of a linear system of algebraic equations.

## Finite Difference Discretisation

Central difference approximations on a uniform grid are used to represent the derivatives of the velocity, pressure and extra stress. The Neumann pressure boundary condition is discretised in the same way. The only implicitness in the algorithm is in the determination of the pressure. This stage requires the solution of a linear system of algebraic equations.

The discretisation of (11) gives rise to a block tridiagonal system for the pressure unknowns in which the diagonal blocks are tridiagonal and the off-diagonal blocks are diagonal. In a pre-processing step an LU decomposition of the matrix is determined and the entries of L and U stored for subsequent use in forward and backward substitution at each time step. It is important to note that this is computationally efficient since the entries of the pressure matrix do not depend on the time step or any other unknowns.

Once the solution has converged the change in fibre direction can be obtained by updating (1) using real time and assuming the terms on the R.H.S. are known.

## Numerical Results

The geometry of the three-dimensional squeeze-film is shown in Figure 1; the planes x = 0, y = 0 and z = 0 are planes of symmetry. We impose no-slip conditions at the top plate, z = Z, and zero normal stresses at the free edges, x = X and y = Y. The dimensions which are used in the program are X = Y = 5 and Z = 0.1 units initially. The velocity of the top plate is taken to be -0.01. The parameters m and n are the grid dimensions, generally taken to be l = 10, m = 10 and n = 10.

The convergence of the numerical scheme was tested for a Newtonian fluid of viscosity 10 and the results compared with the lubrication approximation. The convergence is illustrated in Figures 2-4. Figure 2 shows the dependence of the scheme on the pseudo-time step. For this choice of physical dimensions and viscosity it was found that a maximum time step of $1\times10^{-5}$ was required for the scheme to converge. The smaller the time step the greater number of iterations that are required and the longer the time to converge. For each set of parameters considered there will be an optimum pseudo-time step for convergence and for computational efficiency it is important that a near optimum time step is used. Figures 3 and 4 show the corresponding dependence of the maximum

velocity in the x, y direction and pressure respectively. It can be seen from comparison of Figures 2, 3 and 4 that a tolerance of about $10^{-6}$ is required to obtain converged solutions. The tolerance is defined as the maximum difference of consecutive values of u, v, w or p divided by the maximum value of u, v, w or p respectively, i.e.

$$\max_{u,v,w,p}\left\{\max_{\substack{i=0,l\\ j=0,m\\ k=0,n}}\left\{\frac{u^{n+1}_{i,j,k}-u^{n}_{i,j,k}}{\max\limits_{\substack{i=0,l\\ j=0,m\\ k=0,n}} u^{n+1}_{i,j,k}}\right\},\ \max_{\substack{i=0,l\\ j=0,m\\ k=0,n}}\left\{\frac{v^{n+1}_{i,j,k}-v^{n}_{i,j,k}}{\max\limits_{\substack{i=0,l\\ j=0,m\\ k=0,n}} v^{n+1}_{i,j,k}}\right\},\ \max_{\substack{i=0,l\\ j=0,m\\ k=0,n}}\left\{\frac{w^{n+1}_{i,j,k}-w^{n}_{i,j,k}}{\max\limits_{\substack{i=0,l\\ j=0,m\\ k=0,n}} w^{n+1}_{i,j,k}}\right\},\ \max_{\substack{i=0,l\\ j=0,m\\ k=0,n}}\left\{\frac{p^{n+1}_{i,j,k}-p^{n}_{i,j,k}}{\max\limits_{\substack{i=0,l\\ j=0,m\\ k=0,n}} p^{n+1}_{i,j,k}}\right\}\right\}. \qquad (12)$$

In figure 5 we show some dependencies on grid size. N is taken to be the product of the three components of grid size. It can be shown that the error in the u, v and p calculations is quadratic which confirms the second order accuracy of the finite difference scheme. The percentage error is taken in comparison with the lubrication approximation solution for a Newtonian fluid, as given by Hays [10], which has an accuracy of approximately 0.4%. The memory required is dependent on N and limit of 64Mbytes of core memory restricts the code. This corresponds to a grid size of 21x21x21 and an accuracy of about 1%. The time taken to converge is also dependent on N, as well as on $\Delta t$ and other parameters. This also produces a practical limit for obtaining a solution, i.e. a non-Newtonian solution, with an optimum pseudo time step, which updates **a** ten times will take an approximate minimum of 5 days of real time to run.

Numerical solutions for the fibre-reinforced model characterised by equations (1) to (3) are illustrated in Figures 6 - 11 for a matrix viscosity $\eta_m$ of 10. The fibres are taken to be initially straight and parallel to the x-axis. The orientation vector **a** was updated in real time, using equation (3), in ten real time steps of 0.1; in this time the thickness of the composite is reduced by 10%. For a volume fraction of 0.6 the Christensen formulae (4) and (5) shows that $\eta_T > \eta_L$, i.e. it is easier to shear the composite in the fibre direction than it is in the transverse direction. When squeezing the material it is observed to flow dominantly in the transverse direction with only a small amount of flow in the fibre direction. This would seem to contradict the shear flow prediction. However, if the elongational viscosity is taken into account it can be shown that a suitable choice of the parameter $E_L$ will restrict flow in the fibre direction. Figure 6 shows the maximum velocities in the transverse and longitudinal directions as functions of $E_L$. It can be seen that as $E_L$ reaches $10^7$ very little flow is observed in the fibre direction. This corresponds to a very small change in volume fraction, Figure 7, but a large increase in the force required to maintain squeezing the sample, Figure 8. As can be seen from Figure 7 the change in volume fraction, during the squeezing flow, is small, especially at large $E_L$. Hence, the change in shear viscosities is also small and as $E_L$ increases becomes negligible. Figure 8 shows the increase in the force required to maintain squeezing. This predicts that the inextensibility of the fibres causes resistance to squeezing flow and accounts for the large forces required in experiments to deform the samples, forces much greater than are predicted from the shear flow data. As $E_L$ increases the flow becomes more two-dimensional and the material tends to move only in the transverse direction with a corresponding decrease in the fibre rotation, Figure 9. Figures 10 and 11 show the shape of an initially square sample after compression, for values of $E_L = 10^3$ and $10^7$ respectively. It would seem from the numerical results that $10^6 < E_L < 10^7$ would be consistent with the experimental observations. In practice the elongational viscosity of a composite material is very hard to measure directly and no confirmation of this result is yet to hand.

## Conclusions

In this paper a finite difference method has been presented for the determination of the fibre reorientation in an idealised anisotropic continuum. The shear viscosities dependence on volume fraction have been considered and the dependence on $E_L$ closely examined. It has been shown that the elongational term is very important and it would seem from the numerical results that $E_L = 10$ would be consistent with the experimental observations. The results are in broad agreement with the experimental observations and demonstrate the success of the continuum model to predict flow behaviour.

## References


[1] Ericksen,J.L., Kolloid-Zeitschrift, **173(2)**, 117 (1960)
[2] Rogers,T.G., Composites, **20(1)**, 21 (1989)
[3] Balasubramanyam,R., Jones,R.S., Wheeler,A.B., Composites, **20(1)**, 33 (1989)
[4] Kaprielian,P.V., O'Neill,J.M., Composites, **20(1)**, 43 (1989)
[5] Jones,R.S., Wheeler,A.B., Proc. 3rd European Rheology Conference and Golden Jubilee Meeting of the BSR, 258 (1990)
[6] Bradaigh,C.M.O., Pipes,R.B., Proc. Flow Processes in Composite Materials FPCM '91 (1991)
[7] Chorin,A.J., Maths. Comp., **22**, 745 (1968)
[8] Jones,R.S., Roberts,R.W., Composites, 25(3), **171** (1993)
[9] Christensen,R.M., J. Rheology, **37**, 103 (1993)
[10] Hays, D.F., J. Basic Engng., Trans. ASME, Series D, **85**, 179 (1963)

Figure 1: Geometry of three-dimensional squeeze-film

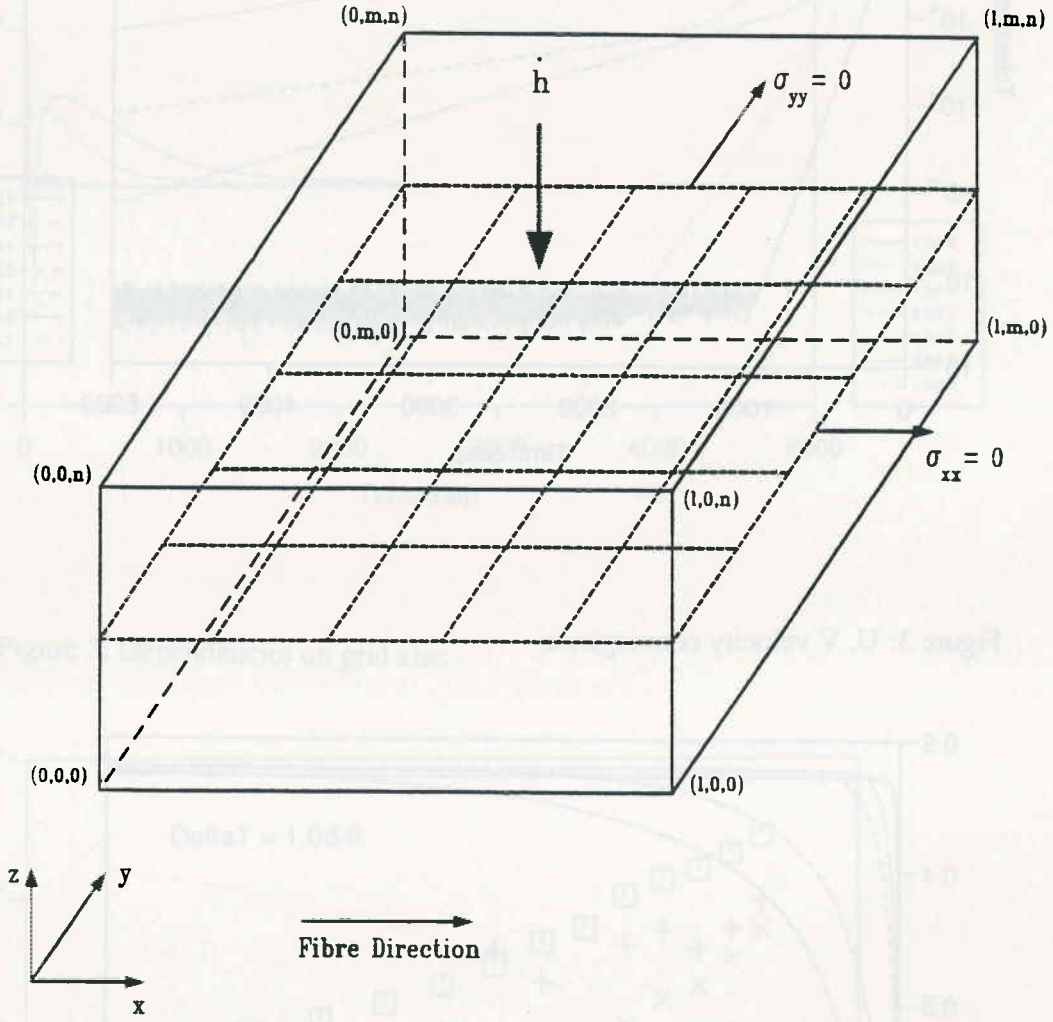

Figure 2: Convergence dependence on Δt

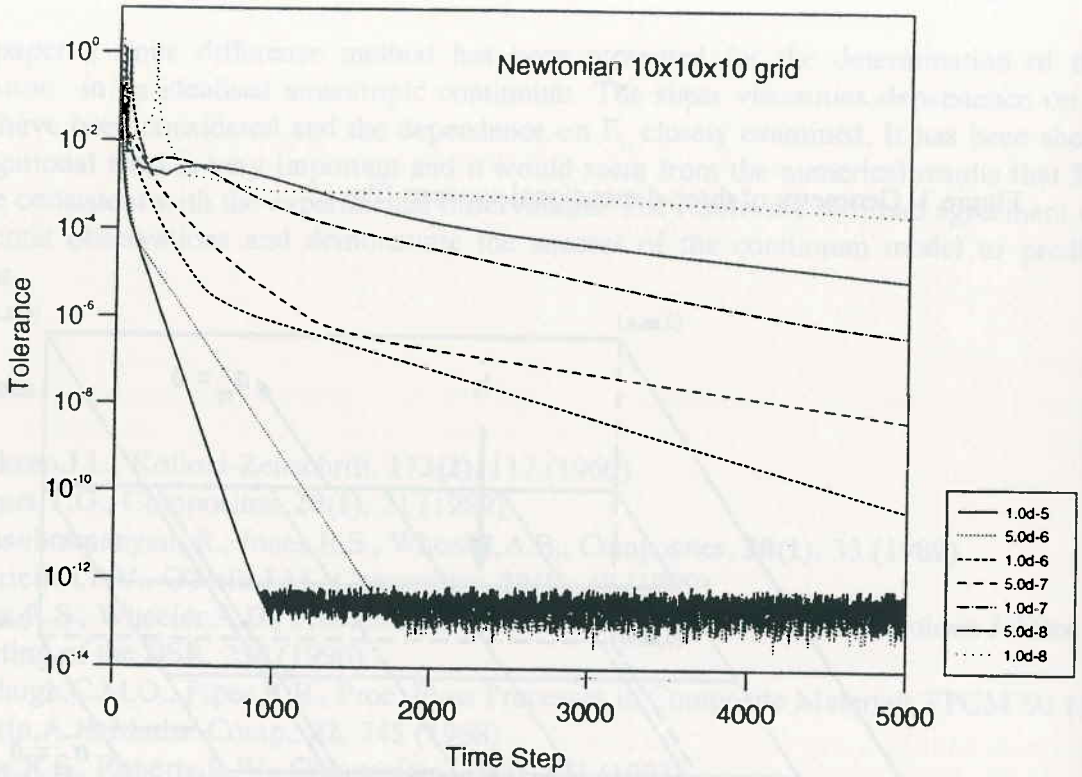


Figure 3: U, V velocity convergence

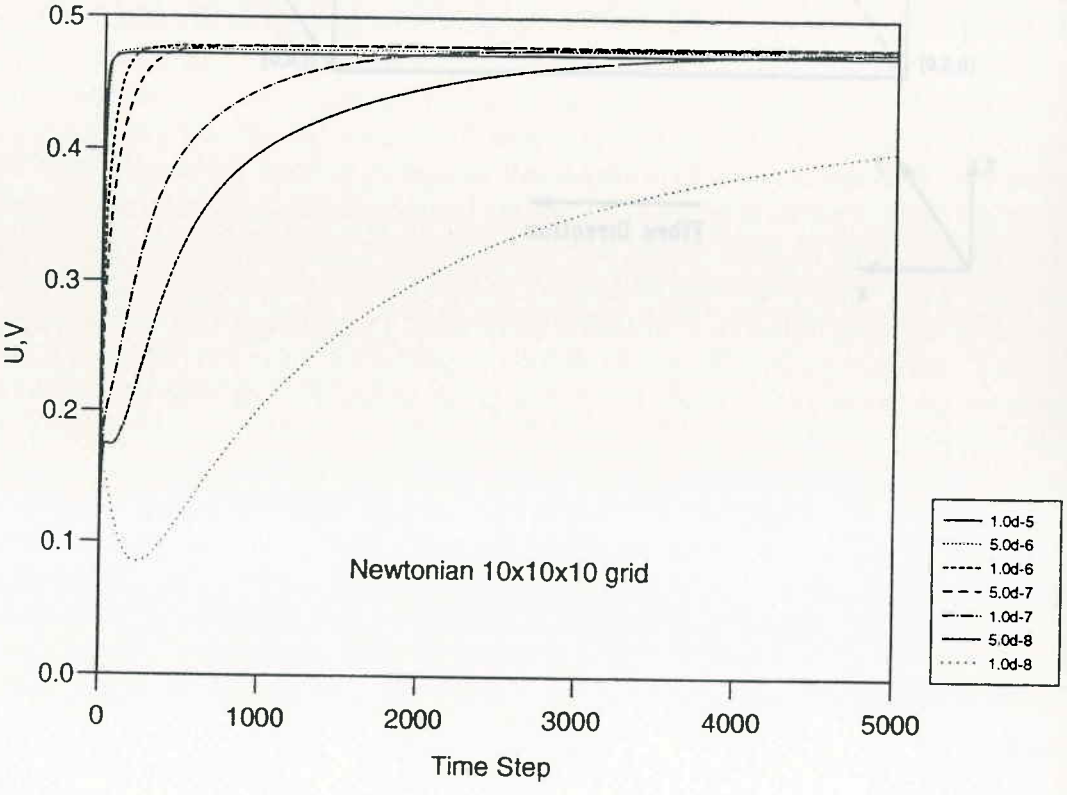

Figure 4: Pressure convergence

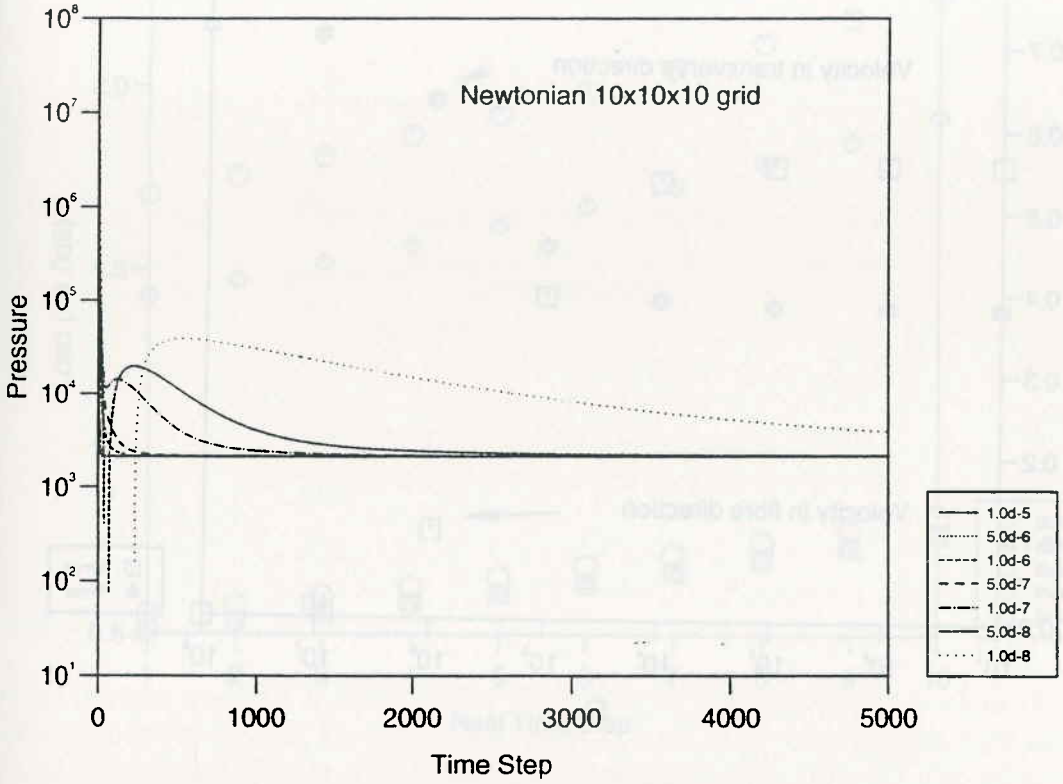


Figure 5: Dependencies on grid size

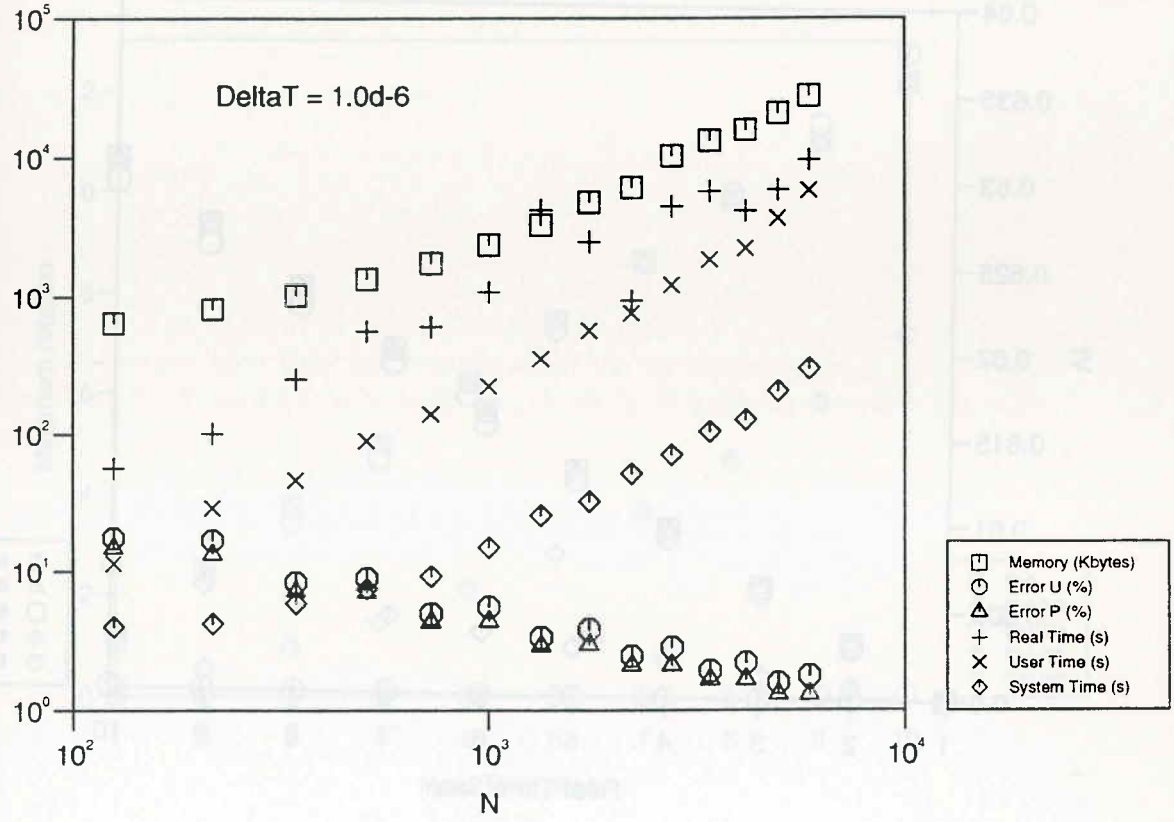

Figure 6: Velocity profile dependence on $E_L$

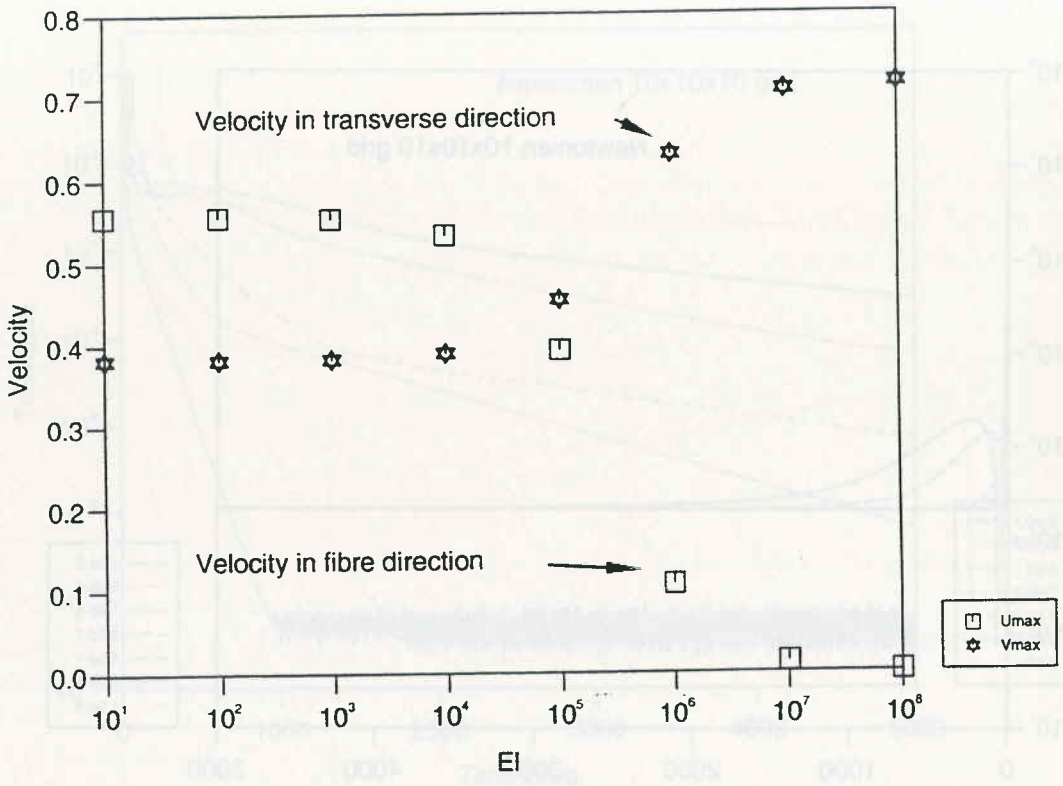


Figure 7: Volume fraction dependence on $E_L$

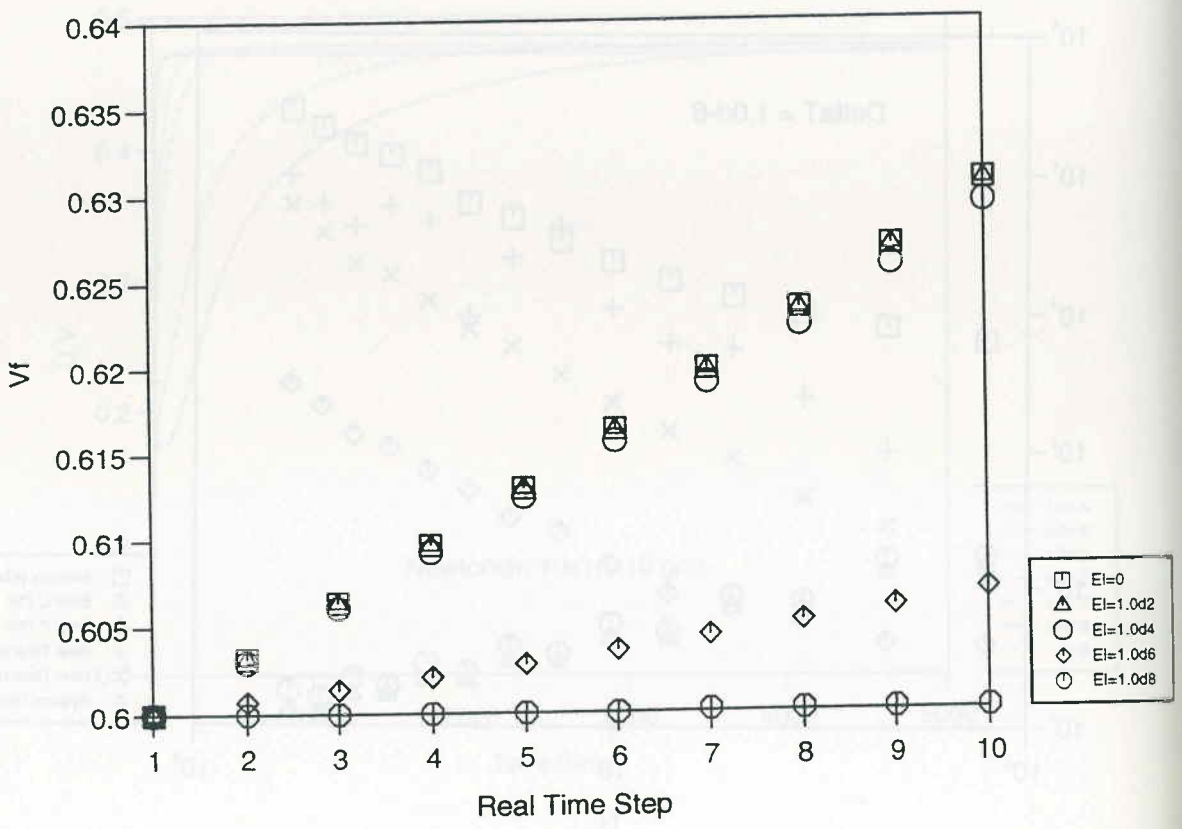

Figure 8: Load dependence on $E_L$

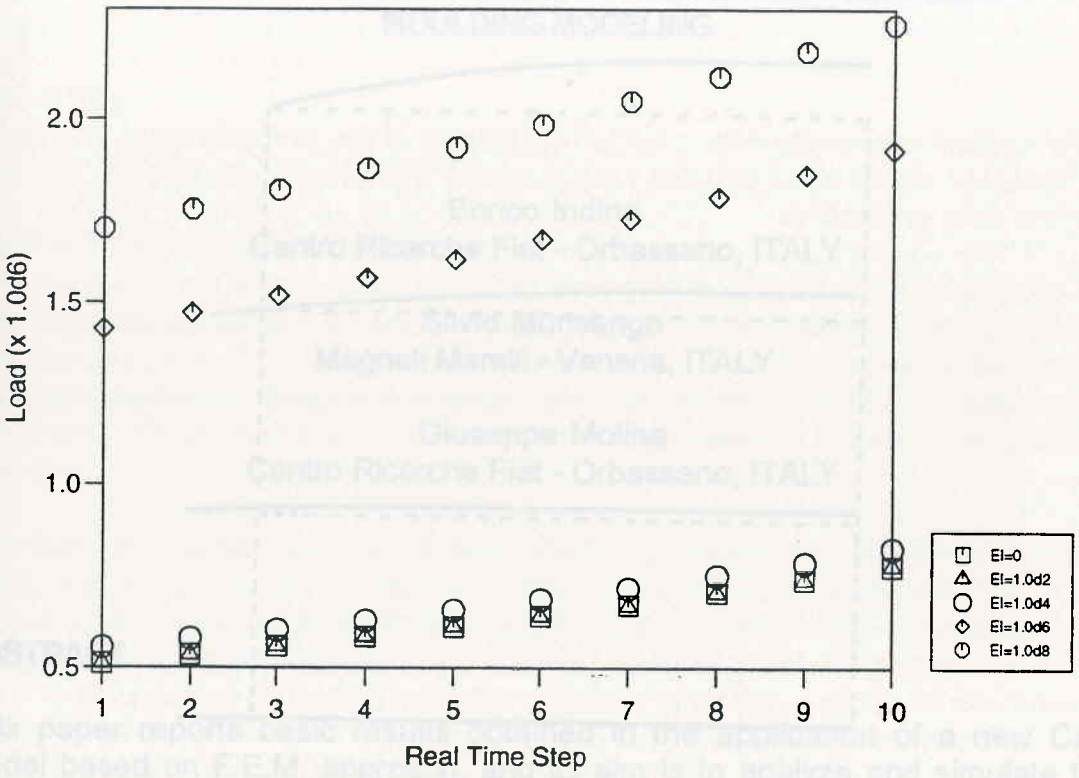


Figure 9: Maximum fibre rotation dependence on $E_L$

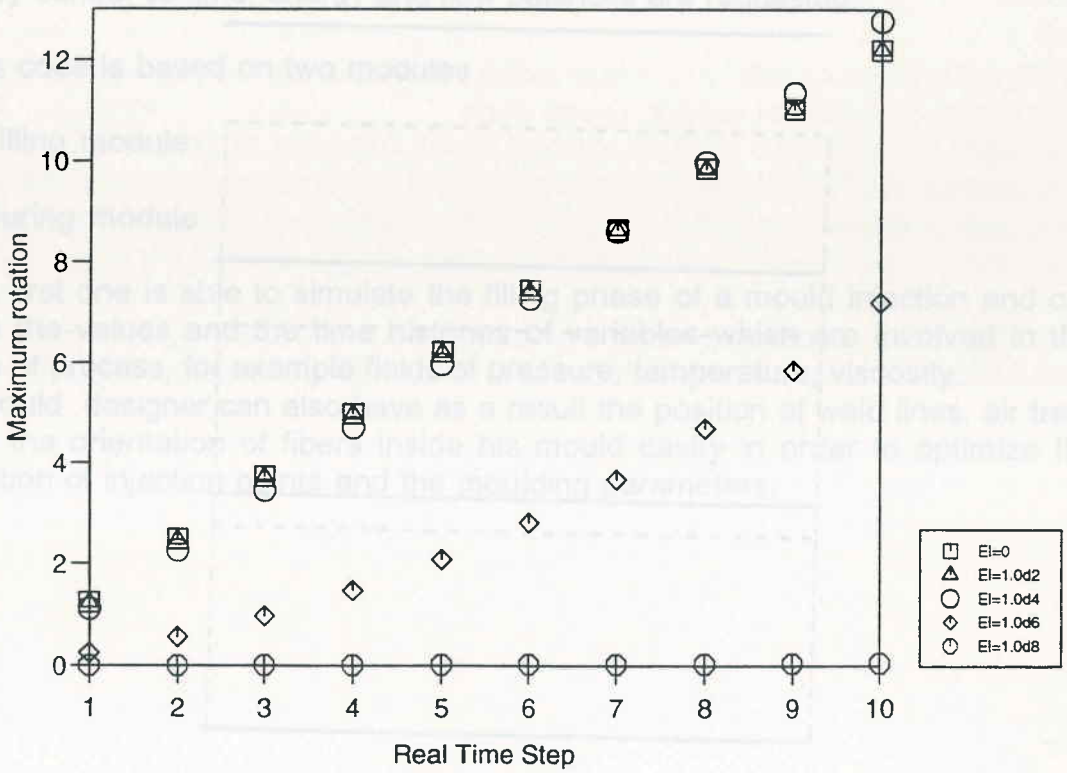

Figure 10: Schematic of fibre movement, $E_L = 1x10^3$

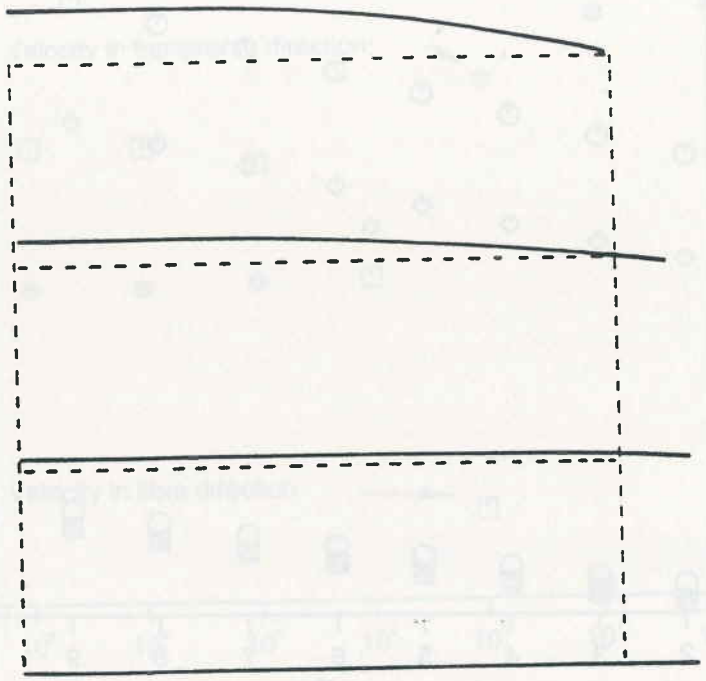

Figure 11: Schematic of fibre movement, $E_L = 1x10^7$